Acta Crystallographica Section A
Foundations of Crystallography
ISSN 0108-7673

Received 22 July 2000
Accepted 24 November 2000

Interference of parametric X-ray and coherent *Bremsstrahlung* radiation from nonrelativistic electrons: application to the phase analysis in crystallography

I. D. Feranchuk[a]* and A. Ulyanenkov[b]

[a]Byelorussian State University, F. Skariny Av. 4, 220050 Minsk, Republic of Belarus, and [b]Bruker AXS, Östlich. Rheinbrückenstrasse 50, 76187 Karlsruhe, Germany. Correspondence e-mail: ilya@fer.minsk.by

The intensity of coherent X-radiation (CXR) from a relativistic electron beam interacting with the crystal [Feranchuk, Ulyanenkov, Harada & Spence (2000). *Phys. Rev. E*, **62**, 4225–4234] is studied in view of its application to the phase determination problem. The analysis of CXR spectra is shown to permit an independent measurement of unit-cell structure factors, defined by both the electron-density distribution and the nucleus positions. In relation to these structure factors, two new types of Patterson function are introduced that can simplify the solution of crystal structure.

1. Introduction

The phase problem is a fundamental problem of crystallography because its solution would help to reconstruct unambiguously the spatial distribution of electron density within the crystal from the intensity distributions of the diffracted waves (Vainshtein, 1981). The development of so-called 'direct methods' for the solution of the phase problem is the cutting edge of both fundamental and applied science (Sanyal *et al.*, 1993; Tegze & Faigel, 1996; Hümmer & Weckert, 1996; Shen, 1999; Iwasaki *et al.*, 1999; Shen *et al.*, 2000*a*,*b*). Brilliant examples of such studies are successful experiments on direct determination of the phases of structure amplitudes by Hümmer & Weckert (1995), Shen (1999) and the reconstruction of X-ray holograms by Bompadre *et al.* (1999).

General trends of development in phase-sensitive diffraction methods are related to the possibility of the *interference of X-ray beams*, which take their origin from different channels of X-ray interaction with atoms in a crystal. In the present report, we discuss a substantially different approach, where the phase information is formed by the *amplitude interference of different mechanisms* of X-ray production by nonrelativistic electrons interacting with the crystal. The interference of amplitudes of different electromagnetic processes initiated by an interaction of charged particles with a media has been discussed (Baryshevskii & Feranchuk, 1983). Two particular mechanisms of X-ray generation within the crystal, parametric X-radiation (PXR) and coherent *Bremsstrahlung* (CBS), have recently been pointed out by Kleiner *et al.* (1994) as candidates for the effective amplitude interference. Experimentally, this effect has been confirmed by Blazhevich *et al.* (1994) and Morokhovskyi *et al.* (2000) for relativistic electrons of energy 5 MeV. Our recent results (Feranchuk & Ulyanenkov, 1999; Feranchuk *et al.*, 2000) demonstrate that the PXR/CBS interference effect is even more prominent for nonrelativistic particles with energies of hundreds of keV when the amplitudes of both processes have the same order of magnitude and interference phenomena result in coherent X-radiation (CXR). Taking this into account allowed us to perform a rigorous theoretical description of experiments by Korobochko *et al.* (1965) and Reese *et al.* (1984), which have not been interpreted correctly for a long time. The results by Feranchuk *et al.* (2000) demonstrate that the phenomenon of PXR/CBS interference opens up new possibilities for the solution of the phase problem in crystallography.

In this paper, we present a detailed analysis of the conditions for the measurement of structure-factor phases using the mentioned interference effect and discuss a possible technique for the realisation of this effect in X-ray structure analysis. The possibility of the phase sensivity of the radiation intensity is based on the differences in the nature of PXR and CBS. Whereas the former arises from the scattering of moving electrons on atomic electrons, the latter is the result of the scattering from both the nuclei and the electrons of the atoms. This difference makes it possible to distinguish the contributions of both modes to the CXR intensity. As a result, two types of structure factor can be determined; the first corresponds to the electron-density distribution and the second describes the location of nuclei inside the crystal elementary cell. On the basis of these structure factors, three types of Patterson function (Buerger, 1959) are introduced and their usage is shown by numerical examples to increase the reso-

lution of Patterson projections and the precision of the reconstructions of the crystalline structure. We also derive the conditions for structure amplitudes, at which their relative phases can be measured and thus the information obtained by other phase-sensitive methods may be complemented.

2. Coherent X-radiation from nonrelativistic electrons in a crystal

We use the following expression from Baryshevskii (1982) for the spectral density of the number of photons emitted in direction $\mathbf{n}$, which takes into account the interaction of both the electron and the electromagnetic field of the emitted photons with the crystal:

$$\mathrm{d}^2N^{(s)}_{\mathbf{n}\omega} = (e^2\omega/4\pi^2c^2)\left|\int_0^{t_L}\mathrm{d}t\,\mathbf{v}(t)\cdot\mathbf{E}_{\mathbf{k}s}(\mathbf{r}(t),\omega)\exp(-i\omega t)\right|^2\mathrm{d}\omega\,\mathrm{d}\mathbf{n}. \tag{1}$$

Here, ω and $\mathbf{k}=\omega/c\mathbf{n}$ are the frequency and wavevector of radiation in the direction $\mathbf{n}$, respectively; $\mathbf{r}(t)$ and $\mathbf{v}(t)$ are the coordinates and the velocity of the electron within the crystal; $\mathbf{E}_{\mathbf{k}s}(\mathbf{r}(t),\omega)$ is the wavefield of the emitted electromagnetic wave with defined polarization, which should be found by taking into consideration the interaction of the wavefield with the crystal; index $s=1,2$ defines one of the polarizations of the emitted photon; $\mathrm{d}\omega$ and $\mathrm{d}\mathbf{n}$ are the spectral and angular intervals where the photons are detected, and t_L represents the time necessary for the electron to cross a crystal of thickness L. Furthermore, we suppose that crystalline films of thicknesses less than the extinction length for emitted photons are used in the experiment, enabling one to find the functions $\mathbf{r}(t)$ and $\mathbf{E}_{\mathbf{k}s}(\mathbf{r},\omega)$ by perturbation theory. It is therefore possible to consider the contribution by different X-ray generation modes to the radiation amplitude additively, as well as to neglect multiple scattering of electrons in the crystal when considering the formation of the coherent radiation peaks.

The electromagnetic field of the emitted radiation under specific diffraction conditions can be written as (Feranchuk & Ulyanenkov, 1999; Nitta, 1991)

$$\begin{aligned}\mathbf{E}_{\mathbf{k}s}(\mathbf{r},\omega) &= \mathbf{e}_s\exp(i\mathbf{k}\cdot\mathbf{r}) + \sum_{\mathbf{g}\neq0}\mathbf{E}_{\mathbf{g}s}\exp[i(\mathbf{k}+\mathbf{g})\cdot\mathbf{r}],\\ \mathbf{E}_{\mathbf{g}s} &= -[\chi_g/(k_g^2-\omega^2/c^2)][\mathbf{k}_g\cdot(\mathbf{g}\cdot\mathbf{e}_s)-\omega^2/c^2\mathbf{e}_s],\\ \mathbf{k}_g &= \mathbf{k}+\mathbf{g},\end{aligned} \tag{2}$$

where $\mathbf{e}_s$ is the polarization vector and χ_g are the Fourier components of the polarizability. The latter describes the *coherent interaction of the emitted radiation* with the periodic charge density of the crystal, and this interaction defines the main properties of parametric X-radiation. The summation in (2) is performed over all reciprocal-lattice vectors (RLV) $\mathbf{g}$ and the volume of the sample equals unity. With the assumption that the radiation frequency is far from the characteristic frequencies of the crystal atoms, the Fourier components of the polarizability can be represented as

$$\chi_g = -\frac{4\pi e^2}{m\omega^2}\frac{S(\mathbf{g})}{\Omega},\quad S(\mathbf{g}) = \sum_i F_i(\mathbf{g})\exp[-W_i(\mathbf{g})]\exp(i\mathbf{g}\cdot\mathbf{R}_i), \tag{3}$$

where e and m are the charge and the mass of the electron; $S(\mathbf{g})$ is the structure factor of the crystal elementary cell of volume Ω, evaluated as a sum of form factors $F_i(\mathbf{g})$ of separate ith atoms at positions $\mathbf{R}_i$; $\exp[-W_i(\mathbf{g})]$ is the Debye–Waller factor taking into account the thermal vibrations of the atoms.

The interaction of electrons and electromagnetic radiation with a crystal leads both to changing the stationary states of the electromagnetic field and to varying the motion law $\mathbf{r}(t)$ of the electron. Meantime, the generation of CBS is caused by the scattering of *electrons* by a coherent periodic potential (Ter-Mikaelian, 1972)

$$\begin{aligned}U(\mathbf{r}) &= (1/\Omega)\sum_{\mathbf{g}\neq0}U_{\mathbf{g}}\exp(i\mathbf{g}\cdot\mathbf{r}),\\ U_{\mathbf{g}} &= 4\pi e\sum_i\exp(i\mathbf{g}\cdot\mathbf{R}_i)\{[Z_i-F_i(\mathbf{g})]/g^2\}\exp[-W_i(\mathbf{g})],\end{aligned} \tag{4}$$

which is defined by the Coulomb interaction of the beam particles both with the electron density of the crystal and with the nuclei. Here Z_i is the charge of the atomic nucleus in the ith position of the crystal unit cell and the other notations have the same meaning as in (3). The law of motion $\mathbf{r}(t)$ of an electron in a potential (4) is given by the solution to Newton equations with an accuracy justified up to $O(U_{\mathbf{g}})$:

$$\begin{aligned}\mathbf{r}(t) &= \mathbf{r}_0+\mathbf{v}_0t+\mathbf{r}_1(t),\\ \mathbf{r}_1(t) &= i(e/m)\sum_{\mathbf{g}}[\mathbf{g}/(\mathbf{g}\cdot\mathbf{v}_0)^2]U_{\mathbf{g}}\exp(i\mathbf{g}\cdot\mathbf{v}_0t),\end{aligned} \tag{5}$$

where the velocity of the electron beam in vacuum is $\mathbf{v}_0$. Then the expression for the radiation intensity in a thin crystal is derived from (1) using (5):

$$\frac{\partial^2N^{(s)}_{\mathbf{n},\omega}}{\partial\omega\partial\mathbf{n}} = \frac{e^2}{4\pi^2c^2}\omega\sum_{\mathbf{g}\neq0}|A_{\mathbf{g}s}(\omega,\mathbf{n})|^2, \tag{6}$$

with the amplitudes $A_{\mathbf{g}s}$ being defined by

$$\begin{aligned}A_{\mathbf{g}s} &= \left\{\mathbf{v}_0\cdot\mathbf{E}_{\mathbf{g}s}-\frac{e}{m}\frac{U_{\mathbf{g}}}{\mathbf{g}\cdot\mathbf{v}_0}\left[\mathbf{e}_s\cdot\mathbf{g}+(\mathbf{e}_s\cdot\mathbf{v}_0)\frac{\mathbf{k}\cdot\mathbf{g}}{\mathbf{g}\cdot\mathbf{v}_0}\right]\right\}Q,\\ Q &= (\sin qL_z/v_0)/q,\quad q=[\omega-\mathbf{v}_0\cdot(\mathbf{k}+\mathbf{g})]/2.\end{aligned} \tag{7}$$

Whereas the first term in (7) describes PXR, the second term determines the coherent *Bremsstrahlung*. The position of the intensity peaks in (7) is defined for both PXR and CBS by the same kinematic factor $|Q|^2$, which appears due to coherent interference of radiation formed by different crystallographic planes. A similar factor was introduced for the kinematical approach to PXR from relativistic electrons by Feranchuk & Ivashin (1985) and the contribution of this factor to radiation intensity is

$$|Q|^2 = 2\pi(L_a/v_0)[1-e^{-L_z/L_a}]\delta[\omega-\mathbf{v}_0\cdot(\mathbf{k}+\mathbf{g})]. \tag{8}$$

Here L_a is the absorption length of the crystal for the frequency determined from the zeros of the δ-function argument in (8). Thus, the distributions of radiation, both spectral and angular, are defined by the sum of resonant terms and,

what is most important, these terms impose equivalent conditions on the frequency and the direction of the emitted photons for both PXR and CBS. For every selected crystallographic reflection with interplane distance d, a set of narrow spectral lines with frequencies $\omega_n(\theta)$ is formed and can be observed in the direction with angle θ to the vector $\mathbf{v}_0$ (Feranchuk & Ulyanenkov, 1999):

$$\omega_n(\theta) = \frac{2\pi v_0 \cos\theta_B}{d(1 - v_0/c\cos\theta)} n, \qquad n = 1, 2, \ldots. \tag{9}$$

The relative width of these lines is proportional to the electron velocity

$$\Delta\omega_0/\omega \approx v_0/L_z\omega_n(\theta), \tag{10}$$

where θ_B is the angle between the velocity $\mathbf{v}_0$ and the normal to the crystallographic planes involved in the scattering process. For nonrelativistic electrons, the number of emitted photons depends weakly on the variation of angle θ. The spectral intensity of photons emitted from one electron in the chosen direction is defined by the sum of the interfering amplitudes of PXR and CBS:

$$\frac{\partial^2 N_s}{\partial\mathbf{n}\partial\omega} = \frac{e^2}{2\pi c^2}\omega_n \frac{L_z}{v_0}|A_{\rm PXR} + A_{\rm CBS}|^2 \delta(\omega - \mathbf{v}_0\cdot(\mathbf{k}+\mathbf{g})), \qquad L_z \le L_a, \tag{11}$$

with amplitudes

$$A_{\rm PXR} = [\chi_g/(k_g^2 - \omega^2/c^2)][(\mathbf{v}_0\cdot\mathbf{k}_g)(\mathbf{g}\cdot\mathbf{e}_s) - \omega^2/c^2(\mathbf{v}_0\cdot\mathbf{e}_s)], \tag{12}$$

$$A_{\rm CBS} = -[eU_g/m\Omega(\mathbf{g}\cdot\mathbf{v}_0)][\mathbf{g}\cdot\mathbf{e}_s + (\mathbf{v}_0\cdot\mathbf{e}_s)(\mathbf{k}\cdot\mathbf{g}/\mathbf{v}_0\mathbf{g})]. \tag{13}$$

The general formulae (11)–(13) demonstrate the explicit dependence of CXR intensity on structure amplitudes, which lays the foundation for the proposed method of phase determination. The method is only usable when the photon detector is able to distinguish the CXR peaks on the incoherent *Bremsstrahlung* background. The results of successful experiments on observation of X-radiation from nonrelativistic electrons in a crystal carried out by Korobochko *et al.* (1965) and Reese *et al.* (1984) prove the possibility of such a separation. Physical parameters of the detector for resolving CXR peaks have been recently discussed by Feranchuk *et al.* (2000).

3. Evaluation of structure amplitudes from CXR spectra

In opposition to the relativistic case, the condition for the position of CXR peaks from nonrelativistic electrons does not fix simultaneously the resonant frequency and the angle of photon emission. This condition, being defined by the argument of the δ function in (11), just establishes the relation between the frequency and the emission angle. Therefore, the CXR peaks can be observed either as angle distribution at fixed radiation frequency or as spectral distribution of photons with fixed detector position. Further, we consider the second experimental scheme (see Fig. 1), which can be realised by positioning the investigated sample immediately on the anode of the X-ray tube (Feranchuk & Ulyanenkov, 1999). Performing the integration over angular detector aperture [see details in Feranchuk *et al.* (2000)] and summing over the polarizations of the emitted photons in (11) by using formula

$$\sum_s e_s^{(\alpha)} e_s^{(\beta)} = \delta_{\alpha,\beta} - k_\alpha k_\beta/k^2,$$

we find that the number of quanta normalized by one electron and registered by the detector is

$$\Delta N(\omega) = \frac{e^2}{2\pi}\omega\frac{L_z}{v}\left[|\mathbf{R}|^2 - \frac{(\mathbf{k}\cdot\mathbf{R})(\mathbf{k}\cdot\mathbf{R}^*)}{k^2}\right]\Phi(\omega-\omega_g). \tag{14}$$

We drop here and in the following equations the index 0 for the electron velocity in vacuum. The function $\Phi(\omega-\omega_g)$ describing the instrumental shape of the CXR peak is determined by detector parameters, angular resolution $\Delta\theta$ and spectral resolution $\Delta\omega$, and does not depend on crystal structure (Feranchuk *et al.*, 2000):

$$\Phi(\omega-\omega_g) = \Delta\theta^2 \exp\{-(\omega-\omega_g)^2/\Delta\omega^2 - (\omega_g v\Delta\theta)^2/[4\Delta\omega^2 c^2(1 - v/c\cos\theta_0)^2]\}. \tag{15}$$

The most essential feature of function Φ for further discussion is its maxima near the characteristic CXR frequencies, the values of which depend on the primary electron velocity v, the observation angle θ_0 and the reciprocal-lattice vectors $\mathbf{g}$ forming the angle θ_B with the electron velocity

$$\omega_g = vg\cos\theta_B/(1 - v/c\cos\theta_0). \tag{16}$$

The radiation intensity dependence on structure amplitudes is defined by the vector

$$\mathbf{R} = \{k\chi_g/[(\mathbf{k}+\mathbf{g})^2 - \omega^2/c^2]\}[\mathbf{g} - \omega/c\mathbf{v}] - [eU_g/m\Omega(\mathbf{g}\cdot\mathbf{v})][\mathbf{g} + \mathbf{v}\omega\cos(\theta_0+\theta_B)/vc\cos\theta_B]. \tag{17}$$

We restrict ourselves to the case when the CXR frequency is far from the anomalous-dispersion region of crystal atoms. Then, according to the definitions for polarizability of crystal (3) and Fourier components of atomic potential (4), two types of structure amplitude can be distinguished in formula (17). Both amplitudes are related to the distribution of charge density inside the crystal unit cell; however, one of them

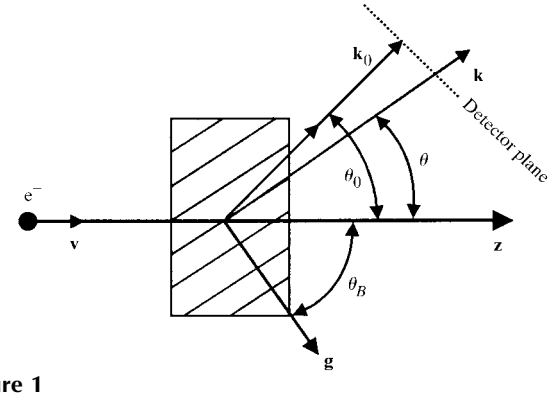

Figure 1
Geometrical sketch of vectors and angles describing the radiation from nonrelativistic electrons in a crystal.

depends on the atomic form factors determined by the electron-density distribution

$$S(\mathbf{g}) = \sum_i F_i(\mathbf{g}) \exp[-W_i(\mathbf{g})] \exp(i\mathbf{g} \cdot \mathbf{R}_i), \tag{18}$$

whereas the second contains the nucleus charges only:

$$S_0(\mathbf{g}) = \sum_i Z_i \exp[-W_i(\mathbf{g})] \exp(i\mathbf{g} \cdot \mathbf{R}_i), \tag{19}$$

thus the spatial distribution of charge density in the latter case is considerably localized and defined by solely nuclear oscillations, which result in the Debye–Waller factor. It should be noted that the structure factor, depending on nucleus positions in the unit cell but not on electron density, appears also in the description of neutron diffraction. However, in this case, it contains poorly defined nuclear scattering lengths (Cowley, 1975) instead of nucleus charges.

Since the radiation intensity (14) contains the considered structure factors along with other physical parameters determining the kinematics of processes, *viz* frequency, velocity and angles, several experimental set-ups can be used for evaluation of the values of S and S_0. A simple experimental scheme for evaluation of structure factors for reciprocal-lattice vector $\mathbf{g}$ could be realised with the measurement of intensity in a CXR peak at several values of some kinematical parameter, *e.g.* velocity (energy) of electrons. Under these conditions, the frequency of radiation is assumed to be constant and equal to ω_g from (16); the function $\Phi(\omega - \omega_g)$ is also replaced by a constant $\Phi_0 = \Phi(0)$, corresponding to the maximum of this function. With these approximations and after some algebra, (14) transforms to the following expression:

$$\begin{aligned}
\Delta N_g = {} & \frac{e^2}{2\pi} \frac{L_z g c^2}{v^2 \cos\theta_B (1 - v/c\cos\theta_0)} \left(\frac{4\pi e^2}{m\Omega g^2 c^2}\right)^2 \Phi_0 \\
& \times \left\{ |S|^2 \frac{(1 - v/c\cos\theta_0)^4}{[1 + v/c\cos(\theta_0 + 2\theta_B)]^2} \right. \\
& \times \left[\sin(\theta_0 + \theta_B) - \frac{v^2 \cos\theta_B \sin\theta_0}{c^2(1 - v/c\cos\theta_0)} \right]^2 \\
& + (|S|^2 + |S_0|^2 - 2|S||S_0|\cos\varphi) \\
& \times \left[\sin(\theta_0 + \theta_B) - \frac{v\cos(\theta_B + \theta_0)\sin\theta_0}{c(1 - v/c\cos\theta_0)} \right]^2 \\
& - 2(|S|^2 - |S||S_0|\cos\varphi) \left[\sin^2(\theta_0 + \theta_B) \right. \\
& + \frac{v\sin(\theta_B + \theta_0)\sin\theta_0[\cos(\theta_B + \theta_0) - v\cos\theta_B]}{c(1 - v/c\cos\theta_0)} \\
& \left. \left. - \frac{v^3 \cos(\theta_B + \theta_0)\cos\theta_B \sin^2\theta_0}{c^3(1 - v/c\cos\theta_0)^2} \right] \right\}.
\end{aligned} \tag{20}$$

The most essential feature in formula (20) is that due to the interference of PXR and CBS; the peak intensity depends not only on the moduli of the structure factors $|S|$ and $|S_0|$ but also on their relative phase φ. The uncommon dependence of the intensity on the electron velocity v^2 should be pointed out as well. The explanation for this behavior is the following: the frequency of the CXR peak for the RLV $\mathbf{g}$ decreases with decreasing electron velocity, which in turn leads to a fast increase of the crystal polarizability and consequently to a quadratic velocity dependence of the intensity.

The intensity variation for different values of structure factors and their relative phases is an important criterion for the effectiveness of the phase-determination methods. The technique proposed in the present work can give substantial separation of observed intensities and dependence on the phase and structure-factor values. Fig. 2 shows the dependence of $v^2/c^2\Delta N$ for $\theta_0 = \theta_B = \pi/4$ on the electron velocity for different ratios of structure-factor modulus $\gamma = |S|/|S_0|$, and the relative phase $\varphi = 0$ (three lower curves). The calculation of $|S_0|$ is straightforward from these data because as the velocity decreases all the curves tend to this value:

$$v^2/c^2 \Delta N_g = \frac{e^2}{2\pi} \frac{L_z g}{\cos\theta_B} \left(\frac{4\pi e^2}{m\Omega g^2 c^2}\right)^2 \Phi_0 |S_0|^2 \sin^2(\theta_0 + \theta_B). \tag{21}$$

However, when the electron velocity v increases, the behavior of curves becomes considerably different for different values of ratio γ. The dashed curves in Fig. 2, showing the intensity dependence on electron velocity for equivalent ratios γ but different phases φ, illustrate phase sensitivity of the X-ray intensity in the framework of the proposed method. In this case, the intensity variation is even larger than for the former case of constant phase. For the particular case of a centrosymmetric crystal, the relative phase can take two values only, $\varphi = 0$ or $\varphi = \pi$ (Buerger, 1959). These two cases are obviously separated in their intensities in Fig. 2. For clarity, the intensity for relative phase $\varphi = \pi/2$ is also depicted, which can be observed for an elementary cell without inversion center.

4. Evaluation of electron density

In this section, we present some examples of supplementary information on crystal structure delivered by the PXR/CBS interference effect. As was shown above, the method permits the estimation of not only the structure-factor modulus $|S(\mathbf{g})|$, which is accessible by conventional X-ray analysis, but also

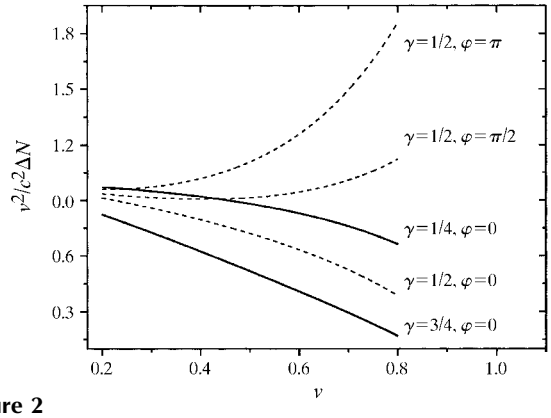

Figure 2
The dependence of value $v^2/c^2\Delta N$ on the electron velocity v for different values of structure-factor ratio γ and phase φ.

two additional characteristics of unit cell in the reciprocal space, determined by the parameter $|S_0(\mathbf{g})|$ and the phase $\varphi(\mathbf{g})$. To clarify the physical meaning of these parameters in direct space, let us assume that they have been evaluated for a large number of RLVs and define the analog of the Patterson function for them (Buerger, 1959):

$$\begin{aligned} P(\mathbf{r}) &= \sum_{\mathbf{g}} |S(\mathbf{g})|^2 \exp(i\mathbf{g}\cdot\mathbf{r}) \\ P_0(\mathbf{r}) &= \sum_{\mathbf{g}} |S_0(\mathbf{g})|^2 \exp(i\mathbf{g}\cdot\mathbf{r}) \\ P_1(\mathbf{r}) &= \sum_{\mathbf{g}} |S(\mathbf{g})||S_0(\mathbf{g})| \cos\varphi(\mathbf{g}) \exp(i\mathbf{g}\cdot\mathbf{r}). \end{aligned} \tag{22}$$

Using the assumption[1] that at low temperature the average amplitude of nucleus oscillations is essentially less than the dimension of atoms within a unit cell, the functions (22) are expressed through the convolutions of charge density in real space:

$$\begin{aligned} P(\mathbf{r}) &= \int \mathrm{d}\mathbf{u} \sum_i \sum_j \rho_i(\mathbf{u}-\mathbf{R}_i)\rho_j(\mathbf{r}-\mathbf{R}_j+\mathbf{u}) \\ P_0(\mathbf{r}) &= \int \mathrm{d}\mathbf{u} \sum_i \sum_j Z_i T_0(\mathbf{u}-\mathbf{R}_i) Z_j T_0(\mathbf{r}-\mathbf{R}_j+\mathbf{u}) \\ P_1(\mathbf{r}) &= \tfrac{1}{2}\sum_i \sum_j Z_i[\rho_j(\mathbf{R}_i-\mathbf{R}_j+\mathbf{r}) + \rho_j(\mathbf{R}_i-\mathbf{R}_j-\mathbf{r})]. \end{aligned} \tag{23}$$

Here, $\rho_i(\mathbf{r}-\mathbf{R}_i)$ is the electron-density distribution in the ith atom with coordinate $\mathbf{R}_i$ and the integration is performed over the entire unit cell. The function $T_0(\mathbf{r}-\mathbf{R}_i)$ describes the 'smearing' of the nuclei in real space caused by their thermal oscillations. In the framework of the approximations used, it weakly depends on the charge of the nucleus and is considerably more localized than the function $\rho(\mathbf{r})$. It is of special importance that the Patterson function P_1 depends linearly on the distribution of electron density, contrary to the classical Patterson function P, which depends on the square of this value. Meanwhile, the peaks of function P_0 are considerably more strongly localized than those of function P, which simplifies the identification of nuclei positions. For illustration of the difference between functions $P_{0,1}$ introduced in the present work and the classical Patterson function P, a numerical example of a one-dimensional crystal with period d and two atoms of charge $Z_{1,2}$ in the unit cell is given below. To derive the final formulae analytically, the electron-density distribution in every atom is assumed to be Gaussian with FWHM $a_{1,2}$, defined by the Thomas–Fermi radius:

$$a_{1,2} = \nu(Z_{1,2})^{-1/3},$$

where ν is constant. The distribution of nuclear density is also described by a Gaussian with FWHM $\Delta \ll a_{1,2}$. Using these approximations, the real-space distributions for electron charge density $\rho(x)$ and for nuclear charge density $\rho_n(x)$ (taking thermal oscillations into account) both defined inside the crystal unit cell are written as

$$\begin{aligned} \rho(x) &= (1/\nu\pi^{1/2})\{(Z_1)^{4/3}\exp[-(x-d/4)^2/a_1^2] \\ &\quad + (Z_2)^{4/3}\exp[-(x+d/4)^2/a_2^2]\} \\ \rho_n(x) &= (1/\Delta\pi^{1/2})\{Z_1\exp[-(x-d/4)^2/\Delta^2] \\ &\quad + Z_2\exp[-(x+d/4)^2/\Delta^2]\}. \end{aligned} \tag{24}$$

Both functions, simulated for the above-mentioned example crystal, are depicted in Fig. 3.

Finally, the classical Patterson function P and the introduced analogous functions P_0 and P_1 for the discussed unit cell are presented:

$$\begin{aligned} P(x) &= [1/\nu(2\pi)^{1/2}]\{(Z_1)^{7/3}\exp(-x^2/2a_1^2) \\ &\quad + (Z_2)^{7/3}\exp(-x^2/2a_2^2)\} + \{Z_1Z_2/[\pi(a_1^2+a_2^2)]^{1/2}\} \\ &\quad \times \{\exp[-(x-d/2)^2/(a_1^2+a_2^2)] \\ &\quad + \exp[-(x+d/2)^2/(a_1^2+a_2^2)]\} \end{aligned} \tag{25}$$

$$\begin{aligned} P_0(x) &= [1/\Delta(2\pi)^{1/2}]\Big((Z_1^2+Z_2^2)\exp(-x^2/2\Delta^2) \\ &\quad + Z_1Z_2\{\exp[-(x-d/2)^2/2\Delta^2] \\ &\quad + \exp[-(x+d/2)^2/2\Delta^2]\}\Big) \end{aligned} \tag{26}$$

$$\begin{aligned} P_1(x) &= (1/\nu\pi^{1/2})\{(Z_1)^{7/3}\exp(-x^2/a_1^2) \\ &\quad + (Z_2)^{7/3}\exp(-x^2/a_2^2)\} + (Z_1Z_2/2a_1\pi^{1/2}) \\ &\quad \times \{\exp[-(x-d/2)^2/a_1^2] + \exp[-(x+d/2)^2/a_1^2]\} \\ &\quad + (Z_1Z_2/2a_2\pi^{1/2})\{\exp[-(x-d/2)^2/a_2^2] \\ &\quad + \exp[-(x+d/2)^2/a_2^2]\}. \end{aligned} \tag{27}$$

Fig. 4 demonstrates the differences between the classical function P and functions P_0 and P_1. These can help in the interpretation of Patterson-function peaks for the solution of crystal structure and electron-density distribution.

The applicability of the proposed approach depends on the volume of reciprocal-lattice space where the relative phases of structure amplitudes $S_0(\mathbf{g})$ and $S(\mathbf{g})$ are not equal to zero. As an example, the analytical formulas are derived below for a crystal with a centrosymmetric unit cell, containing two groups of atoms. Let Z_i represent the charges of atomic group i

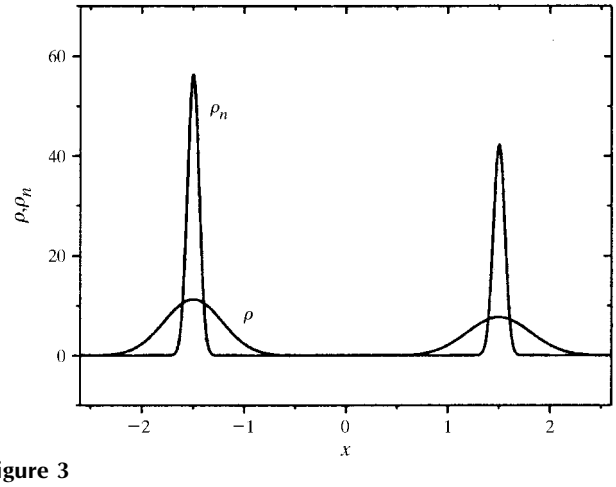

Figure 3
Calculated real-space distributions of electron charge density ρ and nucleus charge density ρ_n taking into account thermal oscillations. The curves are presented within the region of the unit cell with period $d = 5$.

[1] This assumption is also used for the construction of the classical Patterson function (Buerger, 1959).

($i = 1, 2$) and, for distinctness, suppose $Z_1 > Z_2$. If the Debye–Waller factor is neglected, the structure amplitudes can be represented as

$$S(\mathbf{g}) = AF_1(\mathbf{g}) + BF_2(\mathbf{g}), \quad S_0(\mathbf{g}) = AZ_1 + BZ_2.$$

Here, $F_1(\mathbf{g})$, $F_2(\mathbf{g})$ define the form factors of atoms belonging to the first and second groups, respectively. The real values A and B are the structure factors of the cell, depending on the atom coordinates of the corresponding groups:

$$A = \sum \exp i\mathbf{g}\mathbf{R}_j^{(1)}, \quad B = \sum \exp i\mathbf{g}\mathbf{R}_j^{(2)}.$$

Because of the cell's symmetry, both functions $S_0(\mathbf{g})$ and $S(\mathbf{g})$ are real and their relative phase can only take values 0 or π. The relative phase can be non-zero only when the parameters A and B are of opposite sign and satisfy the following inequalities:

$$\frac{Z_1}{Z_2} < \left|\frac{B}{A}\right| < \frac{F_1}{F_2}.$$

The Thomas–Fermi representation of the atom form factor is used below:

$$F(\mathbf{g}) = Z\varphi(\mathbf{g}Z^{-1/3}),$$

where $\varphi(x)$ is a universal monotonically decreasing function normalized with the condition $\varphi(0) = 1$.

Then, for every $Z_1 > Z_2$, the volume of reciprocal-lattice space where structure amplitudes $S_0(\mathbf{g})$ and $S(\mathbf{g})$ are of opposite sign, is not equal to zero and is determined by the inequalities

$$\frac{Z_1}{Z_2} < \left|\frac{B}{A}\right| < \frac{Z_1}{Z_2}\frac{\varphi(\mathbf{g}Z_1^{-1/3})}{\varphi(\mathbf{g}Z_2^{-1/3})}.$$

For the Bragg reflections, which belong to the selected area in reciprocal-lattice space, the method presented in this paper allows one to define the signs of structure amplitudes for centrosymmetric crystals and thus to supplement information delivered by other phase-sensitive methods.

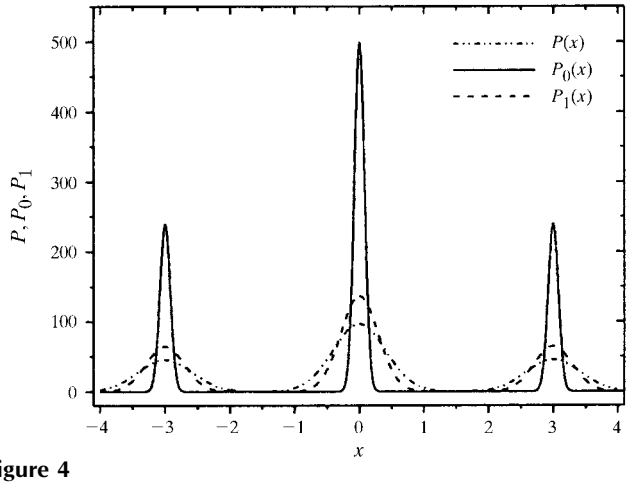

Figure 4
Simulated classical Patterson function P and functions introduced in this work P_0 and P_1 for a crystal of period $d = 6$.

One more possibility that could enhance the capabilities of this method should be mentioned. One can choose the energy of the generated X-radiation in a way that it falls on the anomalous dispersion of one of the cell's atoms. In this situation, the theoretical description should take into account anomalous dispersion and absorption corrections for the amplitude of the electron beam scattering by the atomic electrons. Using the method described by Feranchuk & Ivashin (1989), we derived an expression for CXR intensity for this case (not presented here) and have carried out a qualitative comparison of theoretical predictions with the experimental results from Reese *et al.* (1984). The theory fits fairly well with the general behavior of the experimental curves. However, to obtain quantitative results, this technique requires a high-precision measurements of radiated intensity, which is hampered by the intense background of incoherent *Bremsstrahlung* (Feranchuk *et al.*, 2000) and therefore needs further technical improvements of the experimental set-up. Finally, the experimental conditions (Shen *et al.*, 2000*a*,*b*) providing the phase-sensitive effects in X-ray diffraction are also of great interest in the analysis of CXR spectra.

5. Conclusions

We have shown theoretically that the CXR spectra from nonrelativistic electrons passing through the crystal depend on the relative phases of structure amplitudes within the definite range of the reciprocal-lattice vectors. Analysis of these spectra permits one to supplement the information obtained from another phase-sensitive method and to build two additional Patterson functions, which simplify the problem of reconstruction of the charge-density distribution within the unit cell of the investigated crystal. The advantages of the proposed method and qualitative features of the Patterson functions are illustrated by the numerical examples.

The authors wish to thank Dr R. Eisenhower of Bruker AXS for comments on the manuscript.

References

Baryshevskii, V. G. (1982). *Channelling, Radiation and Reactions in Crystals under High Energies.* Belarussian University, Minsk, Republic of Belarus.
Baryshevskii, V. G. & Feranchuk, I. D. (1983). *J. Phys. (Paris)*, **44**, 913–922.
Blazhevich, S. V., Blochek, G. L., Gavrikov, V. B., Kulibaba, V. I., Maslov, N. I., Nasonov, N. N., Pyrogov, B. H., Safronov, A. G. & Torgovkin, A. V. (1994). *Phys. Lett. A*, **195**, 210–212.
Bompadre, S. G., Petersen, T. W. & Sorensen, L. B. (1999). *Phys. Rev. Lett.* **83**, 2741–2744.
Buerger, M. J. (1959). *Vector Space and its Application in Crystal-Structure Investigation.* New York: Wiley.
Cowley, J. M. (1975). *Diffraction Physics.* New York: American Elsevier.
Feranchuk, I. D. & Ivashin, A. V. (1985). *J. Phys. (Paris)*, **46**, 1981–1986.
Feranchuk, I. D. & Ivashin, A. V. (1989). *Kristallographiya*, **34**, 39–46; Engl. transl: *Sov. Phys. Crystallogr.* **34**, 21–24.
Feranchuk, I. D. & Ulyanenkov, A. (1999). *Acta Cryst.* A**55**, 466–470.

Feranchuk, I. D., Ulyanenkov, A., Harada, J. & Spence, J. C. H. (2000). *Phys. Rev. E*, **62**, 4225–4234.
Hümmer, K. & Weckert, E. (1995). *Acta Cryst.* A**51**, 431–438.
Hümmer, K. & Weckert, E. (1996). *X-ray and Neutron Dynamical Diffraction. NATO Adv. Sci. Inst. Ser.* **357**, 345–368. New York: Plenum Press.
Iwasaki, H., Yurugi, T. & Yoshimura, Y. (1999). *Acta Cryst.* A**55**, 864–870.
Kleiner, V. L., Nasonov, N. N. & Safronov, A. G. (1994). *Phys. Status Solidi B*, **181**, 223–231.
Korobochko, V., Kosmach, V. & Mineev, V. (1965). *Zh. Eksp. Teor. Fiz.* **48**, 1248; Engl. transl: *Sov. Phys. JETP*, **21**, 834–839.
Morokhovskyi, V. V., Freudenberger, J., Genz, H., Morokhovskii, V. L., Richter, A. & Sellschop, J. P. F. (2000). *Phys. Rev. B*, **61**, 3347–3352.
Nitta, H. (1991). *Phys. Lett. A*, **158**, 270–274.
Reese, G. M., Spence, J. C. H. & Yamamoto, N. (1984). *Philos. Mag.* **49**, 697–716.
Sanyal, M. K., Sinha, S. K., Gibaud, A., Huang, K., Carvalho, B., Rafailovich, M., Sokolov, J., Zhao, X. & Zhao, W. (1993). *Europhys. Lett.* **21** 691.
Shen, Q. (1999). *Phys. Rev. B*, **59**, 11109–11112.
Shen, Q., Kycia, S. & Dobrianov, I. (2000*a*). *Acta Cryst.* A**56**, 264–267.
Shen, Q., Kycia, S. & Dobrianov, I. (2000*b*). *Acta Cryst.* A**56**, 268–279.
Tegze, M. & Faigel, G. (1996). *Nature (London)*, **380**, 49–53.
Ter-Mikaelian, M. L. (1972). *High Energy Electromagnetic Processes in Condensed Media.* New York: Wiley.
Vainshtein, B. K. (1981). *Modern Crystallography*. *Springer Series in Solid-State Sciences*, Vol. 15. New York: Springer-Verlag.